



# An inverse method for the estimation of input forces acting on non-linear structural systems

Chih-Kao Ma<sup>a,\*</sup>, Chih-Cherng Ho<sup>b</sup>

<sup>a</sup> *Department of Naval Architecture and Marine Engineering, Chung-Cheng Institute of Technology, Ta-Hsi Taoyuan 33509, Taiwan, ROC*

<sup>b</sup> *Department of System Engineering, Chung-Cheng Institute of Technology, Ta-Hsi Taoyuan 33509, Taiwan, ROC*

Received 24 January 2003; accepted 26 June 2003

## Abstract

This study proposes an inverse method to identify input forces of non-linear structural systems. The method is an extension of the previous work that is limited to linear structural systems. The present estimation method is composed of the extended Kalman filter and a recursive least-squares estimator. By using the inverse method, input forces acting on non-linear structural systems can be estimated from measured dynamic responses. In this work, numerical simulations of input forces estimation of non-linear lumped-mass systems are performed to verify the practicality and accuracy of the proposed algorithm. The simulation results demonstrate that the application of the input force estimation method to non-linear structural systems is successful.

© 2003 Elsevier Ltd. All rights reserved.

## 1. Introduction

For the analysis and design of structural systems, the estimation of real input loads is a very important and necessary task. By way of determining the dynamic loads, many problems such as the strength, fatigue and reliability of structures can be evaluated adequately. However, for some physical systems, direct measurements of excitation forces are difficult to be realized because of very large magnitudes of forces or installation problems of force transducers. Therefore, it is necessary to find alternate methods to estimate input forces. One of the methods is to identify the input forces from measured dynamic responses by an inverse method.

The inverse estimation method is in fact a force identification, which is a process of determining applied loads from dynamic responses of structures. Stevens [1] presented an overview of the force identification process for the case of linear vibration systems, and classified them into discrete systems and continuous systems. Öry et al. [2] used the William's method with a time integration scheme to identify shock loadings. Doyle [3–7] used the frequency domain method to

\*Corresponding author. Tel.: +886-3-380-0958; fax: +886-3-389-2134.

E-mail address: [chihkao@ccit.edu.tw](mailto:chihkao@ccit.edu.tw) (C.-K. Ma).

obtain the time histories of forces from the experimentally measured responses (strains, velocities, etc.). Inoue et al. [8,9] adopted a least-squares method based on singular value decomposition to improve the estimation accuracy of the deconvolution method. A method to minimize the mean square error of the estimation was also presented by them. Wang and Kreitinger [10] employed a direct approach, called the sum of weighted acceleration technique (SWAT), to identify the unknown forces. The SWAT method used the product of measured accelerations and effective or optimal weights to estimate the input forces. Recently, Huang [11] applied the conjugate gradient method (CGM), which is an iterative regularization method, to estimate the external forces of a lumped-mass system with time-dependent parameters.

Take a comprehensive review of the above references, the estimation algorithms are all in batch forms and most of the applications are limited to linear structural systems. However, the non-linearity always exists in real structural systems. For real mechanical or structural systems, the non-linearity appears in various types and is stronger with the increasing response amplitude. In addition, estimating the parameters on-line is necessary to obtain real-time results. Hence, the object of this study is to develop an on-line inverse method, which is capable of identifying input forces for non-linear structural systems. The method is an extension of the input forces estimation method developed in the previous study [12].

This paper first briefly reviews the fundamental equations of lumped-mass structural systems. An on-line extended inverse method of estimating the input forces is then developed. The inverse method comprises the EKF and the RLSE. The accuracy of the proposed method is verified by numerical simulations of input forces estimation of non-linear lumped-mass systems. The direct dynamic responses of structural systems are obtained by Newmark's  $\beta$  method. The proposed algorithm then uses the responses to estimate the corresponding input forces. From the comparisons between the estimated and exact input forces, we can conclude that the proposed algorithm applied successfully in input forces estimation of non-linear structural systems.

## 2. Fundamental equations

### 2.1. Equations of motion

For an  $n$  degree-of-freedom (d.o.f.) lumped-mass structural system, as shown in Fig. 1, the equations of motion can be written as follows:

$$M\ddot{Y}(t) + C\dot{Y}(t) + K(t)Y(t) = F(t), \quad (1)$$

where  $M$  denotes the  $n \times n$  mass matrix,  $C$  the  $n \times n$  damping matrix,  $K$  the  $n \times n$  stiffness matrix,  $F(t)$  the  $n \times 1$  input force vector, and  $\ddot{Y}$ ,  $\dot{Y}$ ,  $Y$  the  $n \times 1$  vectors of acceleration, velocity and displacement, respectively; and

$$M = \begin{bmatrix} m_1 & 0 & 0 & \cdots & 0 \\ 0 & m_2 & 0 & \cdots & 0 \\ 0 & 0 & m_3 & \cdots & 0 \\ \vdots & \vdots & \vdots & \ddots & \vdots \\ 0 & 0 & 0 & \cdots & m_n \end{bmatrix}_{n \times n},$$

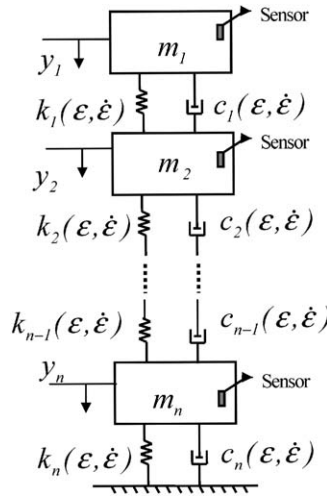


Fig. 1. A non-linear MDOF spring–mass–damper system.

$$\ddot{Y} = \begin{bmatrix} \ddot{y}_1 \\ \ddot{y}_2 \\ \vdots \\ \ddot{y}_n \end{bmatrix}_{n \times 1}, \quad \dot{Y} = \begin{bmatrix} \dot{y}_1 \\ \dot{y}_2 \\ \vdots \\ \dot{y}_n \end{bmatrix}_{n \times 1}, \quad Y = \begin{bmatrix} y_1 \\ y_2 \\ \vdots \\ y_n \end{bmatrix}_{n \times 1}, \quad F = \begin{bmatrix} F_1 \\ F_2 \\ \vdots \\ F_n \end{bmatrix}_{n \times 1}.$$

For linear systems, the viscous damping and spring forces are assumed proportional to velocity and displacement, respectively. However, for non-linear systems, the damping or spring forces are usually expressed as functions of displacements and velocities with higher orders. Hence, elements of the matrices  $C$  and  $K$  will no longer be constants for non-linear systems. The relationships between the resistive forces of spring or damper and the displacements or velocities may be specified through the force-state mapping technique [13].

Assuming that the spring force and damping force can be approximated by analytic functions of the relative displacement and relative velocity, respectively, we then expand the functions in power series forms with respect to these parameters. For a relatively small motion, the higher order terms of the power series can be neglected. In this work, we assume that the resistive forces of the spring and damper are functions of the linear and cubic terms of displacements and velocities, respectively. It means the spring force  $F_s$  and damping force  $F_d$  can be written as

$$F_s = k\varepsilon + k'\varepsilon^3, \tag{2}$$

$$F_d = c\dot{\varepsilon} + c'\dot{\varepsilon}^3, \tag{3}$$

where  $k, k', c$  and  $c'$  are constants,  $\varepsilon$  and  $\dot{\varepsilon}$  denote the relative displacement and velocity between two adjacent lumped masses, respectively. The stiffness matrix  $K$  and the damping matrix  $C$  of a non-linear lumped-mass system can be presented as follows:

$$C = \begin{bmatrix} c_1 + c'_1(\dot{y}_2 - \dot{y}_1)^2 & -c_1 - c'_1(\dot{y}_2 - \dot{y}_1)^2 & 0 & \cdots & 0 & 0 \\ -c_1 - c'_1(\dot{y}_2 - \dot{y}_1)^2 & c_1 + c_2 + c'_1(\dot{y}_2 - \dot{y}_1)^2 + c'_2(\dot{y}_3 - \dot{y}_2)^2 & -c_2 - c'_2(\dot{y}_3 - \dot{y}_2)^2 & \cdots & 0 & 0 \\ 0 & -c_2 - c'_2(\dot{y}_3 - \dot{y}_2)^2 & c_2 + c_3 + c'_2(\dot{y}_3 - \dot{y}_2)^2 + c'_3(\dot{y}_4 - \dot{y}_3)^2 & \cdots & 0 & 0 \\ \vdots & \vdots & \vdots & \ddots & \vdots & \vdots \\ 0 & 0 & 0 & \cdots & \ddots & -c_{n-1} - c'_{n-1}(\dot{y}_n - \dot{y}_{n-1})^2 \\ 0 & 0 & 0 & 0 & -c_{n-1} - c'_{n-1}(\dot{y}_n - \dot{y}_{n-1})^2 & c_{n-1} + c_n + c'_{n-1}(\dot{y}_n - \dot{y}_{n-1})^2 + c'_n \dot{y}_n^2 \end{bmatrix}$$

$$K = \begin{bmatrix} k_1 + k'_1(y_2 - y_1)^2 & -k_1 - k'_1(y_2 - y_1)^2 & 0 & \cdots & 0 & 0 \\ -k_1 - k'_1(y_2 - y_1)^2 & k_1 + k_2 + k'_1(y_2 - y_1)^2 + k'_2(y_3 - y_2)^2 & -k_2 - k'_2(y_3 - y_2)^2 & \cdots & 0 & 0 \\ 0 & -k_2 - k'_2(y_3 - y_2)^2 & k_1 + k_2 + k'_1(y_2 - y_1)^2 + k'_2(y_3 - y_2)^2 & \cdots & 0 & 0 \\ \vdots & \vdots & \vdots & \ddots & \vdots & \vdots \\ 0 & 0 & 0 & \cdots & \ddots & -k_{n-1} - k'_{n-1}(y_n - y_{n-1})^2 \\ 0 & 0 & 0 & 0 & -k_{n-1} - k'_{n-1}(y_n - y_{n-1})^2 & k_{n-1} + k_n + k'_{n-1}(y_n - y_{n-1})^2 + k'_n y_n^2 \end{bmatrix}$$

## 2.2. Direct analysis of dynamic responses

The Newmark's  $\beta$  method is used to predict the responses of non-linear lumped-mass structures acting by dynamic loadings. Considering the simplicity and efficiency, we adopt the constant average acceleration method (i.e.,  $\beta = \frac{1}{4}$ ). The method is a forward integration in time domain and unconditionally stable. In terms of the incremental equations of motion, the responses can be computed step by step as follows [14]:

$$K_D = K(Y(t), \dot{Y}(t)) + \frac{2}{\Delta t}C(Y(t), \dot{Y}(t)) + \frac{4}{\Delta t^2}M, \quad (4)$$

$$F_D = \Delta F + 2C(Y(t), \dot{Y}(t)) + M\frac{4}{\Delta t}\dot{Y}(t) + M2\ddot{Y}(t), \quad (5)$$

$$\Delta Y = K_D^{-1}F_D, \quad (6)$$

$$Y(t + \Delta t) = Y(t) + \Delta Y, \quad (7)$$

$$\dot{Y}(t + \Delta t) = \frac{2}{\Delta t}\Delta Y - \dot{Y}(t), \quad (8)$$

$$\ddot{Y}(t + \Delta t) = \frac{4}{\Delta t^2}\Delta Y - \frac{4}{\Delta t}\dot{Y}(t) - \ddot{Y}(t + \Delta t), \quad (9)$$

where  $K_D$ ,  $F_D$ ,  $\Delta F$ ,  $\Delta Y$ ,  $\Delta t$  are dynamic stiffness matrix, equivalent dynamic load matrix, incremental force matrix, incremental displacement matrix and incremental time, respectively. In the present study, the sum of the calculated dynamic response and a pseudo-white noise is used to simulate the really measured response and investigate the influence of the measurement noise on input forces estimation.

## 3. Inverse analysis of input forces

### 3.1. Application of the extended Kalman filter (EKF)

The EKF, whose essential idea was proposed by Schmidt, is a form of the Kalman filter [15] "extended" to non-linear dynamic systems [16]. For a non-linear model, the EKF linearizes the model around the current state, and applies the Kalman filter to the resulting time varying linear model. It is a robust modelling approach under the existence of noise. In fact, the EKF technique has been widely used in many fields of science and engineering [17,18].

To estimate the states of non-linear systems through the EKF, we first transform the equations of motion into the state equations. The transformation can be achieved by selecting the state vector  $X(t) = [Y(t), \dot{Y}(t)]^T$ . According to Eq. (1), the continuous-time state and measurement equations can be written as

$$\dot{X}(t) = A(t)X(t) + BF(t) = f(X, F), \quad (10)$$

$$Z(t) = HX(t) = h(X), \quad (11)$$

where

$$A(t) = \begin{bmatrix} 0_{n \times n} & I_{n \times n} \\ -M^{-1}K(Y) & -M^{-1}C(\dot{Y}) \end{bmatrix}, \quad B = \begin{bmatrix} 0_{n \times n} \\ M^{-1} \end{bmatrix},$$

$$H = [I_{n \times n} \quad 0_{n \times n}],$$

$$X(t) = [x_1(t) \quad x_2(t) \quad \cdots \quad x_{2n-1}(t) \quad x_{2n}(t)]^T,$$

$$F(t) = [F_1(t) \quad F_2(t) \quad \cdots \quad F_{n-1}(t) \quad F_n(t)]^T.$$

Here, Eqs. (10) and (11) are linearized around the nominal state  $X^*(t)$  and nominal input  $F^*(t)$ , which are obtained in terms of the EKF predictor equation. Then, the linearized equations are discretized over time intervals of length  $\Delta T$ . Considering the uncertainties and disturbances in the real physical world, the input process and measurement noises are added into the linearized state and measurement equations, respectively. The discrete-time form of the linearized state and measurement equations are shown as follows:

$$X(k + 1) = \Phi X(k) + \Gamma(F(k) + w(k)), \tag{12}$$

$$Z(k + 1) = HX(k + 1) + v(k + 1), \tag{13}$$

$$\Phi = I + \frac{\partial f(X^*(k), F^*(k))}{\partial X} \Delta T,$$

$$\Gamma = \frac{\partial f(X^*(k), F^*(k))}{\partial F} \Delta T,$$

$$H = \frac{\partial h(X^*(k), F^*(k))}{\partial X} \Delta T,$$

$$F(k) = [F_1(k) \quad F_2(k) \quad \cdots \quad F_{n-1}(k) \quad F_n(k)],$$

$$Z(k) = [z_1(k) \quad z_2(k) \quad \cdots \quad z_{n-1}(k) \quad z_n(k)],$$

$$w(k) = [w_1(k) \quad w_2(k) \quad \cdots \quad w_{n-1}(k) \quad w_n(k)],$$

$$v(k + 1) = [v_1(k + 1) \quad v_2(k + 1) \quad \cdots \quad v_{n-1}(k + 1) \quad v_n(k + 1)],$$

where  $X(k)$  is the state vector,  $F(k)$  the sequence of deterministic input,  $\Delta T$  the sampling time interval,  $Z(k)$  the observation vector. The process noise vector  $w(k)$  is assumed to be zero mean and white with variance  $E\{w(k)w(j)^T\} = Q\delta_{kj}$ . Here,  $\delta_{kj}$  is the Kronecker delta. The measurement noise vector  $v(k)$  is also assumed to be zero mean and white. The variance of  $v(k)$  is given by  $E\{v(k)v(j)^T\} = R\delta_{kj}$ . Here,  $R = \sigma^2$  and  $\sigma$  represents the standard deviation of the measurement noise. The matrices  $\Phi$ ,  $\Gamma$ , and  $H$  are the Jacobians with respect to the state vector or the input force vector, evaluated in the estimated values.

### 3.2. The recursive input estimation approach

In the previous section, the discrete-time state equations of a non-linear MDOF lumped-mass system excited by dynamic loads have been derived. The magnitudes of the unknown input loads can be estimated by an inverse method from the noisy measurements of the system responses. For non-linear structural systems, the inverse method consists of two parts; one is the EKF with no input terms and the other is a recursive least-squares estimator. The equations of the EKF are

$$\bar{X}(k/k-1) = \bar{X}(k-1/k-1) + \int_{t=(k-1)\Delta T}^{t=k\Delta T} f(\bar{X}(k-1/k-1), k-1) dt, \quad (14)$$

$$\Phi = I + \frac{\partial f(\bar{X}(k-1/k-1), k-1)}{\partial X} \Delta T, \quad (15)$$

$$\Gamma = \frac{\partial f(\bar{X}(k-1/k-1), k-1)}{\partial F} \Delta T, \quad (16)$$

$$H = \frac{\partial h(\bar{X}(k/k-1), k-1)}{\partial X} \Delta T, \quad (17)$$

$$P(k/k-1) = \Phi P(k-1/k-1) \Phi^T + \Gamma Q \Gamma^T, \quad (18)$$

$$\bar{Z}(k) = Z(k) - H \Phi \bar{X}(k-1/k-1), \quad (19)$$

$$S(k) = H P(k/k-1) H^T + R, \quad (20)$$

$$K_a(k) = P(k/k-1) H^T S^{-1}(k), \quad (21)$$

$$P(k/k) = [I - K_a(k) H] P(k/k-1), \quad (22)$$

$$\bar{X}(k/k) = \Phi \bar{X}(k/k-1) + K_a(k) \bar{Z}(k). \quad (23)$$

The equations of the recursive least-squares estimator are

$$B_s(k) = H[\Phi M_s(k-1) + I] \Gamma, \quad (24)$$

$$M_s(k) = [I - K_a(k) H][\Phi M_s(k-1) + I], \quad (25)$$

$$K_b(k) = \gamma^{-1}(k) P_b(k) B_s^T(k) [\gamma^{-1}(k) B_s(k) P_b(k-1) B_s^T(k) + S(k)]^{-1}, \quad (26)$$

$$P_b(k) = \gamma^{-1}(k) [I - K_b(k) B_s(k)] P_b(k-1), \quad (27)$$

$$\hat{F}(k) = \hat{F}(k-1) + K_b(k) [\bar{Z}(k) - B_s(k) \hat{F}(k-1)], \quad (28)$$

where  $P$  is the filter’s error covariance matrix,  $S(k)$  the innovation covariance,  $K_a(k)$  Kalman gain,  $B_s(k)$  and  $M_s(k)$  the sensitivity matrices,  $\bar{Z}(k)$  the innovation,  $K_b(k)$  the correction gain for updating  $\hat{F}(k)$ ,  $P_b(k)$  the error covariance of the estimated input vector, and  $\hat{F}(k)$  the estimated input vector. The fading factor  $\gamma(k)$  is employed to compromise between the fast tracking capability and the loss of estimate accuracy. In this study, the adaptive weighting method developed in Tuan and Hou [19] is used to select a suitable  $\gamma(k)$ . That is

$$\gamma(k) = \begin{cases} 1, & |\bar{Z}(k)| \leq \sigma, \\ \frac{\sigma}{|\bar{Z}(k)|}, & |\bar{Z}(k)| > \sigma. \end{cases} \quad (29)$$

Thus, the computational procedure for the estimation of input forces acting on non-linear lumped-mass systems is summarized as follows:

*Step 1:* Derive the system equations of motion (Eq. (1)) and obtain the simulated responses  $Z(k)$  by Newmark’s  $\beta$  method, i.e., Eqs. (4)–(9).

*Step 2:* Use the EKF prediction equation (Eq. (14)) and linearization equations (Eqs. (15)–(17)) to obtain the instant system matrices  $\Phi$ ,  $\Gamma$  and  $H$ .

*Step 3:* Use the rest of the EKF equations, i.e., Eqs. (18)–(22), to generate the innovation covariance  $S(k)$ , innovation  $\bar{Z}(k)$ , and Kalman gain  $K_a(k)$ .

*Step 4:* Use the EKF correction equation, i.e., Eq. (23), to obtain the estimated state vector  $\bar{X}(k/k)$  which is used as the nominal state for the next time step.

*Step 5:* Use the recursive least-squares estimator, i.e., Eqs. (24)–(28), to compute the unknown input forces  $\hat{F}(k)$ .

#### 4. Numerical simulations and discussion

To verify the practicability and accuracy of the proposed approach, numerical simulations are performed on non-linear lumped-mass systems. For simplicity, the spring and damping forces are taken the forms shown in Eqs. (2) and (3), respectively. The system responses are obtained by Newmark’s  $\beta = \frac{1}{4}$  method with the considerations of process and measurement noises. Then, the simulated responses are loaded into the proposed inverse algorithm to estimate the corresponding input forces. The initial conditions of the error covariances are given as  $P(-1/-1) = 10^{10} \times I_{n \times n}$  for the EKF and  $P_b(-1/-1) = 10^8 \times I_{n \times n}$  for the recursive least-squares estimator.

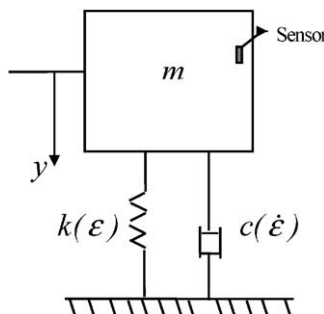


Fig. 2. A non-linear SDOF spring–mass–damper system.



4.1. Numerical simulation example 1

A non-linear single d.o.f. lumped-mass system, as shown in Fig. 2, is considered. The input force with triangular, rectangular, half-sine impulses and mixed configurations is given as

$$F(t) = \begin{cases} 0 \text{ (N)}, & 0 \leq t \leq 0.015 \text{ (s)}, \\ 5 \times 10^7 \times (0.02 - t) \text{ (N)}, & 0.015 < t \leq 0.02 \text{ (s)}, \\ 0 \text{ (N)}, & 0.02 < t \leq 0.025 \text{ (s)}, \\ 2.5 \times 10^5 \text{ (N)}, & 0.025 < t \leq 0.03 \text{ (s)}, \\ 0 \text{ (N)}, & 0.03 < t \leq 0.035 \text{ (s)}, \\ 2.5 \times 10^5 \times \sin(\frac{\pi}{5}(t - 0.035)) \text{ (N)}, & 0.035 < t \leq 0.04 \text{ (s)}, \\ 0 \text{ (N)}, & 0.04 < t \leq 0.045 \text{ (s)}, \\ 2.5 \times 10^5 \times \sin(\frac{\pi}{5}(t - 0.045)) \text{ (N)}, & 0.045 < t \leq 0.0475 \text{ (s)}, \\ 1.25 \times 10^5 \text{ (N)}, & 0.0475 < t \leq 0.05 \text{ (s)}, \\ 0 \text{ (N)}, & 0.05 < t \leq 0.055 \text{ (s)}, \\ 2.5 \times 10^5 \times \sin(\frac{\pi}{5}(t - 0.055)) \text{ (N)}, & 0.055 < t \leq 0.075 \text{ (s)}, \\ 0 \text{ (N)}, & 0.075 < t \leq 0.08 \text{ (s)}. \end{cases}$$

The simulation conditions and the system parameters are given as the following: null initial conditions,  $m = 0.5 \text{ kg}$ ,  $c = 3 \text{ N s m}^{-1}$ ,  $k = 12 \text{ N m}^{-1}$ ,  $k' = 60 \text{ N m}^{-1}$ , sampling time interval  $\Delta T = 1 \times 10^{-5} \text{ s}$ , covariance of process noise  $Q = Q_w \times I_{1 \times 1}$ ,  $Q_w = 1 \times 10^{-6}$ , covariance of measurement noise  $R = \sigma^2 \times I_{1 \times 1}$ ,  $\sigma = 1 \times 10^{-6}$  (see Fig. 3). Fig. 4 depicts the time history of the displacement of the SDOF non-linear system. The noise is about 2% of the displacement. The time histories of the estimated and exact input forces are shown in Fig. 5. The overall relative error  $Er_o$  is used to quantify the deviation between the estimated and exact input forces. The  $Er_o$  is

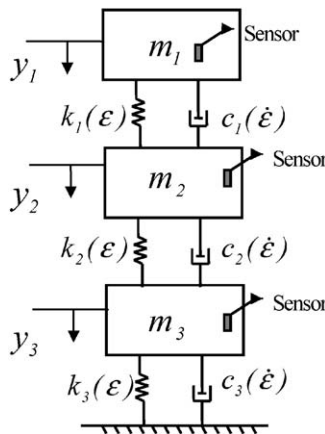


Fig. 3. A non-linear 3-d.o.f. spring–mass–damper system.

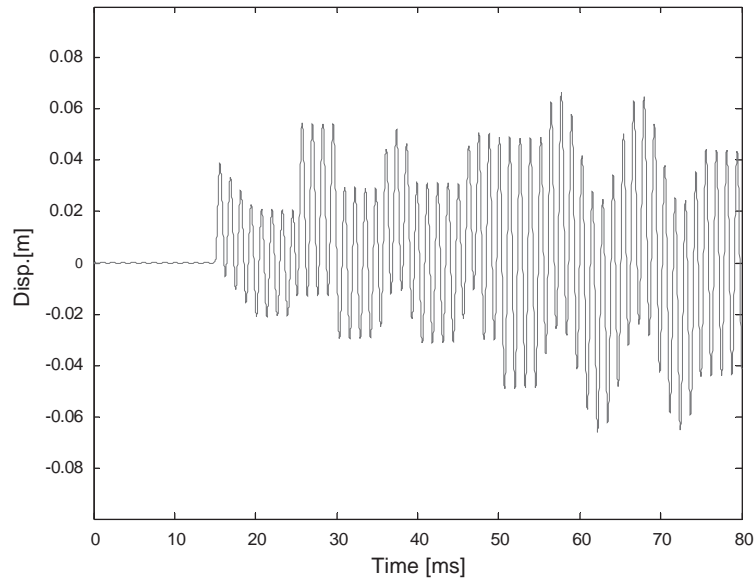


Fig. 4. Time history of the simulated displacement of the non-linear SDOF lumped-mass system ( $k' = 60 \text{ N m}^{-1}$ ;  $\sigma = 10^{-6}$ ;  $Q = 10^{-6}$ ).

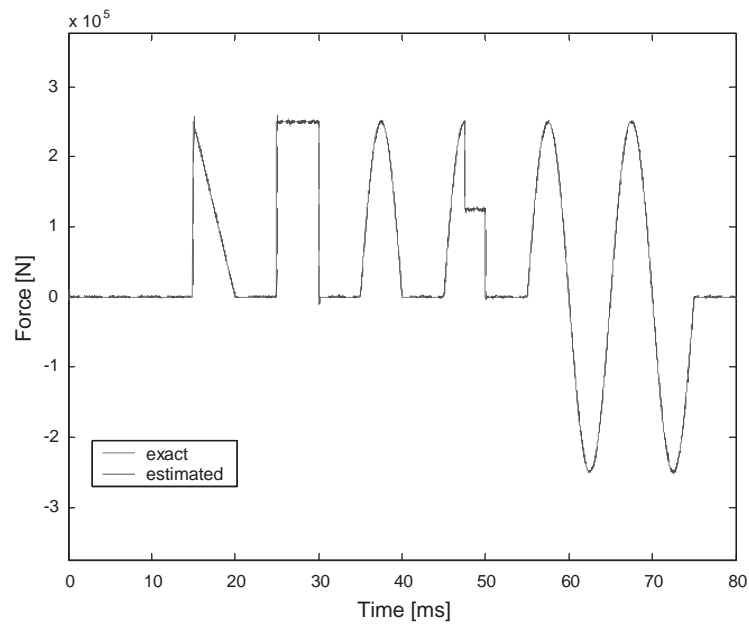


Fig. 5. Time histories of the estimated and exact input forces of the non-linear SDOF lumped-mass system ( $k' = 60 \text{ N m}^{-1}$ ;  $\sigma = 10^{-6}$ ;  $Q = 10^{-6}$ ).

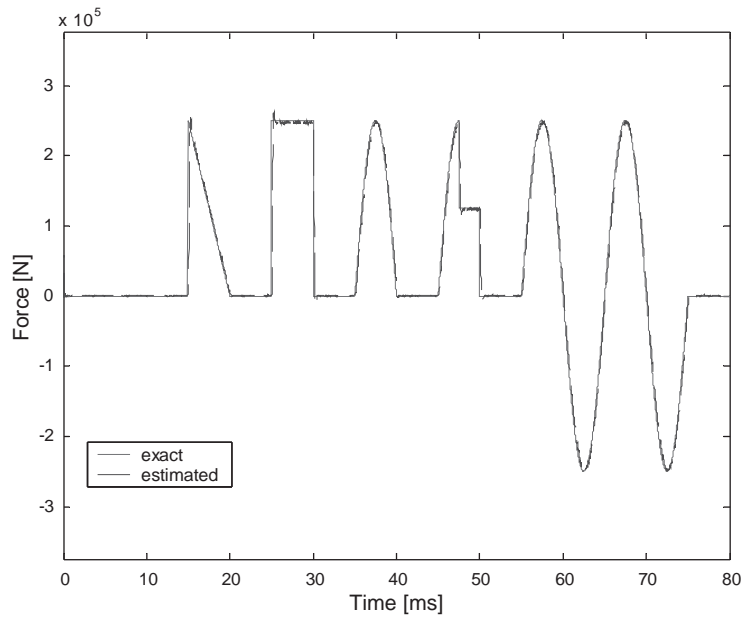


Fig. 6. Time histories of the estimated and exact input forces of the non-linear SDOF lumped-mass system ( $k' = 60 \text{ N m}^{-1}$ ;  $\sigma = 10^{-5}$ ;  $Q = 10^{-6}$ ).

defined as

$$Er_o = \frac{\sum_{k=1}^N |F(k) - \hat{F}(k)|}{\sum_{k=1}^N |F(k)|}, \tag{30}$$

where  $F(k)$  and  $\hat{F}(k)$  designate the exact and estimated forces at time  $t_k$ , respectively, and  $N$  is the sampling number. In order to measure the maximum overshoot or undershoot of local maximum amplitudes of the estimated input forces, another kind of relative error, denoted as  $Er_m$ , is defined as

$$Er_m = \frac{\max |F(l) - \hat{F}(l)|}{|F(l)|}, \tag{31}$$

where  $F(l)$  and  $\hat{F}(l)$  represent the local maximum amplitudes of the exact and estimated input forces, respectively. The above two kinds of relative errors are both used as the performance evaluations in the numerical experiments. For the non-linear SDOF lumped-mass system, the  $Er_o$  of the estimated input force is within 2.53% and the  $Er_m$  of the estimated maximum amplitude is within 3.73%.

In order to investigate the influences of the process and measurement noises, we first change the measurement noise from  $\sigma = 10^{-6}$  to  $10^{-5}$  and keep the value of  $Q_w$  invariant. The estimation result is displayed in Fig. 6. Due to the large measurement noise covariance, the errors  $Er_o$  and  $Er_m$  of the estimated input forces increase to 6.61% and 5.14%, respectively. Next, the process noise is enlarged from  $Q_w = 10^{-6}$  to  $10^{-4}$  with fixed measurement noise. The estimation result of the input force is shown in Fig. 7. It is obvious that the fluctuation of the time history of the estimated input force is increased. Finally, Fig. 8 depicts the estimation results with  $Q_w = 10^{-4}$  and  $\sigma = 10^{-5}$ . The relative errors of the estimation result with different  $Q_w$  and  $\sigma$  values are summarized in Table 1.

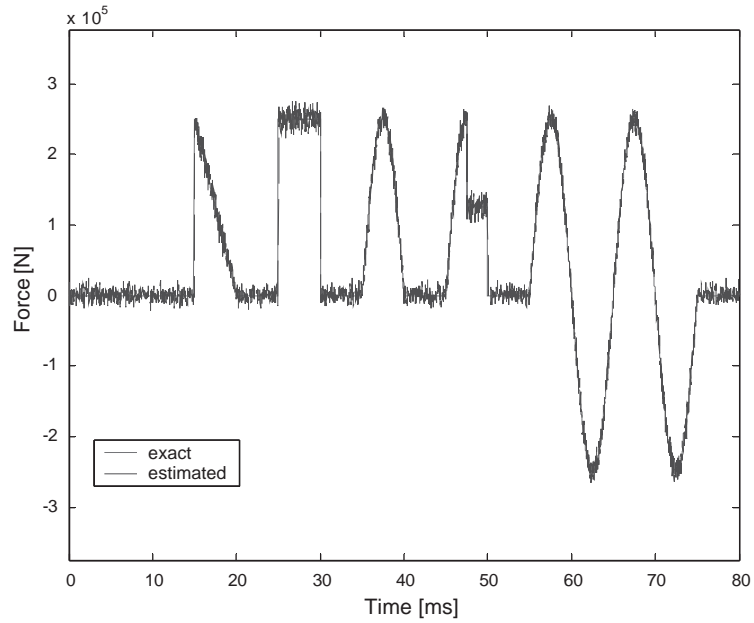


Fig. 7. Time histories of the estimated and exact input forces of the non-linear SDOF lumped-mass system ( $k' = 60 \text{ N m}^{-1}$ ;  $\sigma = 10^{-6}$ ;  $Q = 10^{-4}$ ).

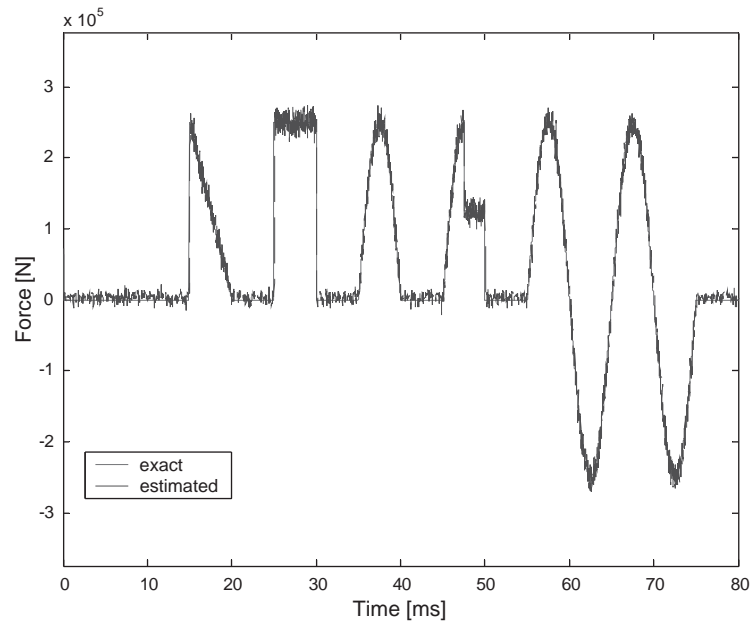


Fig. 8. Time histories of the estimated and exact input forces of the non-linear SDOF lumped-mass system ( $k' = 60 \text{ N m}^{-1}$ ;  $\sigma = 10^{-5}$ ;  $Q = 10^{-4}$ ).

Table 1  
Relative errors of the estimated input force of the non-linear SDOF lumped-mass system

$k'$	$\sigma (R = \sigma^2)$	$Q_w$	Relative error ( $Er_m$ ) (%)	Relative error ( $Er_o$ ) (%)
60 N m <sup>-1</sup>	10 <sup>-6</sup>	10 <sup>-6</sup>	3.73	2.53
60 N m <sup>-1</sup>	10 <sup>-5</sup>	10 <sup>-6</sup>	5.14	6.61
60 N m <sup>-1</sup>	10 <sup>-6</sup>	10 <sup>-4</sup>	11.45	7.43
60 N m <sup>-1</sup>	10 <sup>-5</sup>	10 <sup>-4</sup>	12.13	8.41
1200 N m <sup>-1</sup>	10 <sup>-6</sup>	10 <sup>-6</sup>	3.81	2.83

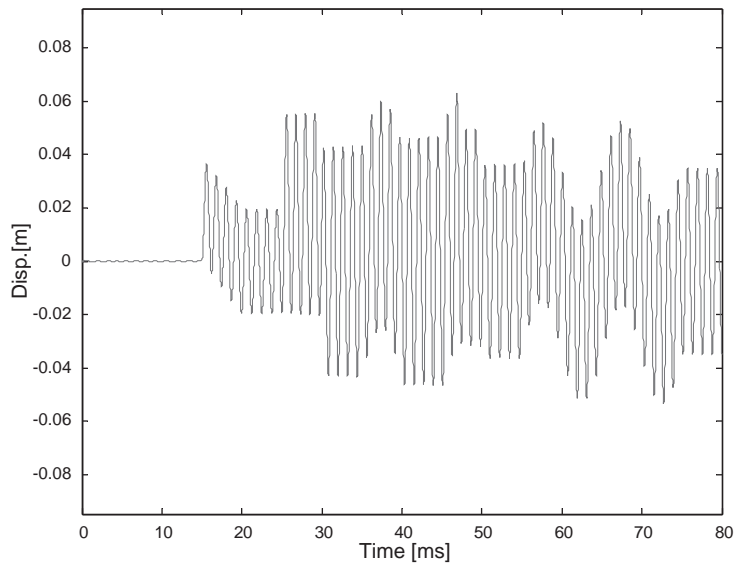


Fig. 9. Time history of the simulated displacement of the non-linear SDOF lumped-mass system ( $k' = 1200 \text{ N m}^{-1}$ ;  $\sigma = 10^{-6}$ ;  $Q = 10^{-6}$ ).

4.2. Numerical simulation example 2

In the second example, the previous SDOF non-linear system is still considered. However, the non-linear spring constant  $k'$  is increased to  $1200 \text{ N m}^{-1}$ . The simulation conditions, system parameters and the input force are same as example 1. Fig. 9 displays the time history of the simulated displacement of the SDOF non-linear system. The noise is about 10% of the displacement. Fig. 10 shows the time histories of the exact and estimated input forces. The relative errors of the estimated input force are also listed in Table 1.

4.3. Numerical simulation example 3

In the last example, a non-linear 3-d.o.f. lumped-mass system, as shown in Fig. 3, is used to verify the proposed inverse method. The parameter values of the 3-d.o.f. system are:

$$m_1 = 40, \quad m_2 = 200, \quad \text{and} \quad m_3 = 300 \text{ (kg)}$$

$$c_1 = 2.5, \quad c_2 = 0.4, \quad \text{and} \quad c_3 = 3.6 \text{ (N s m}^{-1}\text{)},$$

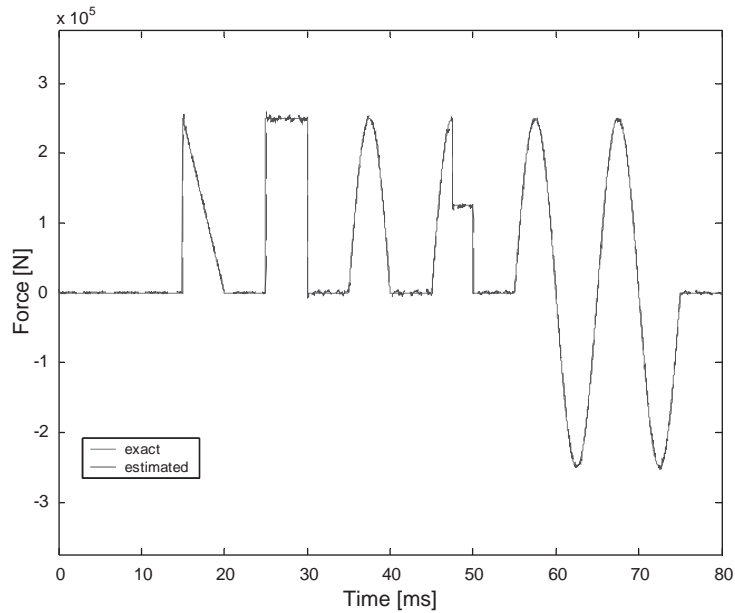


Fig. 10. Time histories of the estimated and exact input forces of the non-linear SDOF lumped-mass system ( $k' = 1200 \text{ N m}^{-1}$ ;  $\sigma = 10^{-6}$ ;  $Q = 10^{-6}$ ).

$$c'_1 = 250, \quad c'_2 = 40, \quad \text{and} \quad c'_3 = 360 \text{ (N s m}^{-1}\text{)},$$

$$k_1 = 3 \times 10^5, \quad k_2 = 8 \times 10^4, \quad \text{and} \quad k_3 = 8 \times 10^5 \text{ (N m}^{-1}\text{)},$$

$$k'_1 = 6 \times 10^7, \quad k'_2 = 1.6 \times 10^7, \quad \text{and} \quad k'_3 = 1.6 \times 10^8 \text{ (N m}^{-1}\text{)}.$$

The simulation conditions are taken as: null initial conditions, sampling interval  $\Delta T = 5 \times 10^{-5} \text{ s}$ , covariance of process noise  $Q = Q_w \times I_{3 \times 3}$ ,  $Q_w = 1 \times 10^{-8}$ , and covariance of measurement noise  $R = \sigma^2 \times I_{3 \times 3}$ ,  $\sigma = 1 \times 10^{-8}$ . In this numerical experiment, three input forces, i.e.  $F_1$ ,  $F_2$  and  $F_3$ , are assumed to act on mass 1, mass 2 and mass 3, respectively. The three input forces are assumed as

$$F_1(t) = \begin{cases} 0 \text{ (N)}, & 0 \leq t \leq 0.015 \text{ (s)}, \\ 2.5 \times 10^5 \text{ (N)}, & 0.015 < t \leq 0.02 \text{ (s)}, \\ 0 \text{ (N)}, & 0.02 < t \leq 0.08 \text{ (s)}, \end{cases}$$

$$F_2(t) = \begin{cases} 0 \text{ (N)}, & 0 \leq t \leq 0.025 \text{ (s)}, \\ 2.5 \times 10^5 \times \sin\left(\frac{\pi}{5}(t - 0.025)\right) \text{ (N)}, & 0.025 < t \leq 0.08 \text{ (s)}, \end{cases}$$

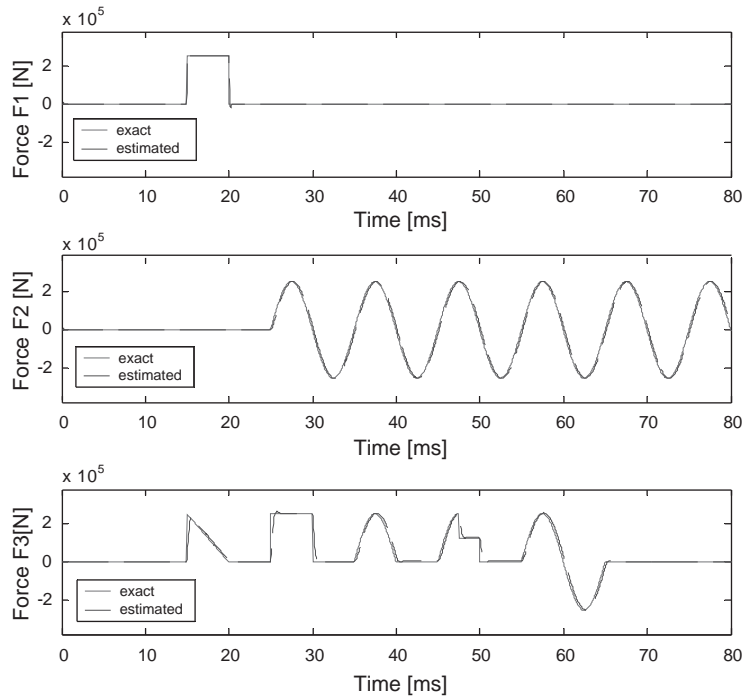


Fig. 11. Time histories of the estimated and exact input forces of the non-linear 3-d.o.f. lumped-mass system ( $\sigma = 10^{-8}$ ;  $Q(1, 1) = 10^{-8}$ ;  $Q(2, 2) = 10^{-8}$ ;  $Q(3, 3) = 10^{-8}$ ).

$$F_3(t) = \begin{cases} 0 \text{ (N)}, & 0 \leq t \leq 0.015 \text{ (s)}, \\ 5 \times 10^7 \times (0.02 - t) \text{ (N)}, & 0.015 < t \leq 0.02 \text{ (s)}, \\ 0 \text{ (N)}, & 0.02 < t \leq 0.025 \text{ (s)}, \\ 2.5 \times 10^5 \text{ (N)}, & 0.025 < t \leq 0.03 \text{ (s)}, \\ 0 \text{ (N)}, & 0.03 < t \leq 0.035 \text{ (s)}, \\ 2.5 \times 10^5 \times \sin(\frac{\pi}{5}(t - 0.035)) \text{ (N)}, & 0.035 < t \leq 0.04 \text{ (s)}, \\ 0 \text{ (N)}, & 0.04 < t \leq 0.045 \text{ (s)}, \\ 2.5 \times 10^5 \times \sin(\frac{\pi}{5}(t - 0.045)) \text{ (N)}, & 0.045 < t \leq 0.0475 \text{ (s)}, \\ 1.25 \times 10^5 \text{ (N)}, & 0.0475 < t \leq 0.05 \text{ (s)}, \\ 0 \text{ (N)}, & 0.05 < t \leq 0.055 \text{ (s)}, \\ 2.5 \times 10^5 \times \sin(\frac{\pi}{5}(t - 0.055)) \text{ (N)}, & 0.055 < t \leq 0.065 \text{ (s)}, \\ 0 \text{ (N)}, & 0.065 < t \leq 0.08 \text{ (s)}. \end{cases}$$

Fig. 11 shows the time histories of the exact and estimated input forces. Table 2 displays the relative errors of the maximum amplitude and the overall relative errors of the three estimated input forces. Next, we tune the values of the process noise covariance  $Q$  to improve the accuracy of the estimation results. The diagonal elements of the matrix  $Q$  are taken as:  $Q(1, 1) = 1 \times 10^{-8}$ ,  $Q(2, 2) = 20 \times 10^{-8}$ ,  $Q(3, 3) = 50 \times 10^{-8}$ . The time histories of the exact and estimated input

Table 2  
Relative errors of the estimated input forces of the non-linear 3d.o.f. lumped-mass system

$\sigma$	$Q$			Relative error ( $Er_m$ ) (%)			Relative error ( $Er_o$ ) (%)		
	$Q(1, 1)$	$Q(2, 2)$	$Q(3, 3)$	$F_1$	$F_2$	$F_3$	$F_1$	$F_2$	$F_3$
$1 \times 10^{-8}$	$1 \times 10^{-8}$	$1 \times 10^{-8}$	$1 \times 10^{-8}$	6.31	0.11	4.76	3.26	9.93	14.14
$1 \times 10^{-8}$	$1 \times 10^{-8}$	$20 \times 10^{-8}$	$50 \times 10^{-8}$	6.29	0.33	6.42	3.25	3.35	5.27

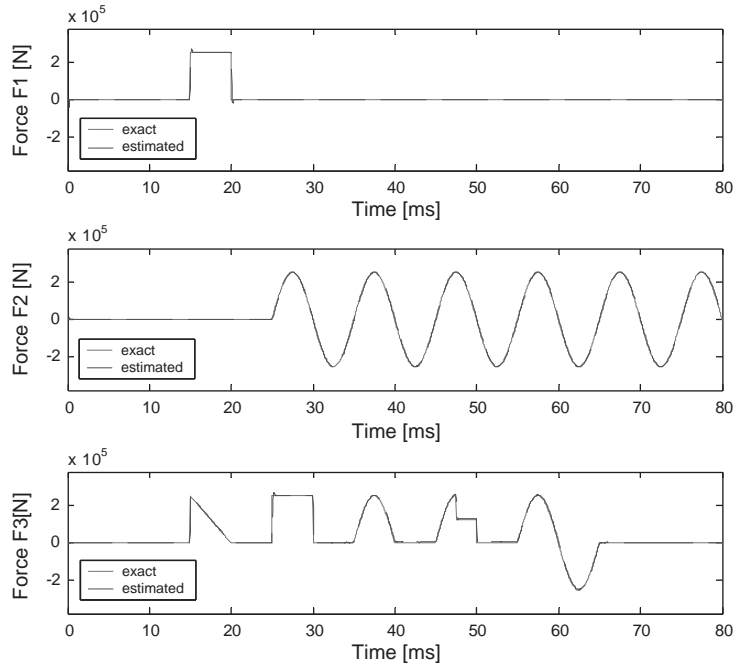


Fig. 12. Time histories of the estimated and exact input forces of the non-linear 3-d.o.f. lumped-mass system ( $\sigma = 10^{-8}$ ;  $Q(1, 1) = 1 \times 10^{-8}$ ;  $Q(2, 2) = 20 \times 10^{-8}$ ;  $Q(3, 3) = 50 \times 10^{-8}$ ).

forces are depicted in Fig. 12. The relative errors  $Er_o$  and  $Er_m$  of the estimated input forces are summarized in Table 2.

4.4. Discussion

- (1) As illustrated in Figs. 5–8 and Figs. 10–12, the estimated input forces converge to their actual values in only few time steps. This is due to the employments of rather large values of error covariances  $P(-1/-1)$  and  $P_b(-1)$  such that the errors of initial estimations can be corrected rapidly.
- (2) From the results in Table 1, we can find that variations of  $Q$  and  $R$  will have large effects on the relative errors  $Er_o$  and  $Er_m$ . In general, large measurement and process noises will both degrade the estimation performance of the proposed algorithm. However, the present inverse method still has a good tracking capability to identify input forces of non-linear lumped-mass systems.



- (3) In Figs. 6 and 7, the estimation results are different from each other because of the selections of different  $Q$  and  $R$  values. Evidently, the estimation result of the input force in Fig. 7 is worse than the result in Fig. 6. However, the difference between the two overall relative errors  $Er_o$  is small, as indicated in Table 1. On the other hand, the difference between the two errors  $Er_m$  is large. This demonstrates that the consideration of the two kinds of relative errors ( $Er_m$  and  $Er_o$ ) is more adequate for the evaluation of the estimation performance.
- (4) The errors  $Er_o$  and  $Er_m$  in example 2 are larger than those in example 1, as indicated in Fig. 5, Fig. 10 and Table 1. The cause is that the stronger non-linearity will induce large linearization errors. The estimation result in example 2 shows that the present inverse method can estimate input forces acting on structural systems with very strong non-linearity.
- (5) Commonly, the measurement noise covariance  $R$  can be specified on the precision of the sensor. The process noise covariance  $Q$  is usually tuned to obtain better estimation results. The proper values of  $Q$  are related to the system modelling error, which is difficult to know prior to the estimation. The optimal tune parameters  $Q$  vary due to the dynamic characteristic of each individual system. Hence, the diagonal elements of the covariance matrix  $Q$  should not be the same for the system with different system parameters. In simulation example 3, we tune the values of  $Q$  with a given value of  $R$ . In terms of adjusting the values of the diagonal elements of the process noise covariance matrix  $Q$ , the accuracy of the estimation results can be improved, as indicated in Figs. 11 and 12 and Table 2.
- (6) Figs. 11 and 12 illustrate that the applicability of the present inverse method facilitates to estimate the input forces of non-linear systems with multiple inputs and multiple outputs. Moreover, even though the input forces estimation algorithm developed in this paper is only applied to non-linear lumped-mass structural systems, it can readily be extended to other types of non-linear structural systems.

## 5. Conclusions

An inverse method to estimate input forces of non-linear structural systems is presented. The approach comprises two parts: the extended Kalman filter and a recursive least-squares estimator. The estimation performance of the proposed method is evaluated through numerical experiments of non-linear lumped-mass systems. The simulation results demonstrate that the present on-line inverse method has been successfully applied to identify the excitation forces. The estimated input forces are qualitatively and quantitatively good in all test cases as long as tuning parameters  $Q$  and  $R$  are chosen adequately. The input force estimation algorithm for two or three-dimensional non-linear structural systems is under development. Future work on this study will also include the application of real-time vibration control of non-linear dynamic systems.

## Appendix A. Nomenclature

$A$	constant matrix
$B$	constant matrix
$B_s$	sensitivity matrices
$C$	damping matrix

$F$	input force vector (the unknown inputs to be estimated)
$H$	measurement matrix
$I$	identity matrix
$k$	time (discretized)
$K$	stiffness matrix
$K_a$	Kalman gain
$k_b$	correction gain
$M$	mass matrix
$M_s$	sensitivity matrices
$P$	filter's error covariance matrix
$P_b$	error covariance matrix
$Q$	process noise covariance matrix
$Q_w$	scalar of process noise covariance
$R$	measurement noise covariance matrix
$R_v$	measurement noise covariance
$S$	innovation covariance
$t$	time (continuous)
$v$	measurement noise vector
$w$	process noise vector
$X$	state vector
$Y$	displacement vector
$\dot{Y}$	velocity vector
$\ddot{Y}$	acceleration vector
$Z$	observation vector
$\gamma$	fading factor
$\Gamma$	input matrix
$\delta$	Kronecker delta
$\Delta T$	sampling time
$\Delta t$	incremental time
$\sigma$	standard deviation
$\Phi$	state transition matrix
$\varepsilon$	relative displacement
$\dot{\varepsilon}$	relative displacement rate
$y$	displacement
$\dot{y}$	velocity
$\ddot{y}$	acceleration
$m$	mass
$k$	stiffness constant of the linear term
$k'$	stiffness constant of the non-linear (cubic) term
$c$	damping constant of the linear term
$c'$	damping constant of the non-linear (cubic) term

### *Superscripts*

$\wedge$	estimated
----------	-----------

–	estimated by filter
T	transpose of matrix
*	nominal

*Subscripts*

*i, j* indices

**References**

- [1] K.K. Stevens, Force identification problems—an overview, *Proceedings of the 1987 SEM Spring Conference on Experimental Mechanics*, Houston, TX, USA, 1987, pp. 14–19.
- [2] H. Öry, H. Glaser, D. Holzdeppe, Quality of modal analysis and reconstruction of forcing functions based on measured output data, *Proceedings of the Fourth IMAC*, Los Angeles, CA, USA, 1986, pp. 850–857.
- [3] J.F. Doyle, Further developments in determining the dynamic contact law, *Experimental Mechanics* 24 (1984) 265–270.
- [4] J.F. Doyle, Determining the contact force during the transverse impact of plates, *Experimental Mechanics* 27 (1987) 68–72.
- [5] J.F. Doyle, Force identification from dynamic responses of a bimaterial beam, *Experimental Mechanics* 33 (1993) 64–69.
- [6] J.F. Doyle, A wavelet deconvolution method for impact force identification, *Experimental Mechanics* 37 (1997) 403–408.
- [7] M.T. Martin, J.F. Doyle, Impact force identification from wave propagation responses, *International Journal of Impact Engineering* 18 (1996) 65–77.
- [8] H. Inoue, N. Ikeda, K. Kishimoto, T. Shibuya, T. Koizumi, Inverse analysis of the magnitude and direction of impact force, *Japan Society of Mechanical Engineers, International Journal Series A* 38 (1995) 84–91.
- [9] H. Inoue, K. Kishimoto, T. Shibuya, T. Koizumi, Estimation of impact load by inverse analysis, *Japan Society of Mechanical Engineers, International Journal Series I* 35 (1992) 420–427.
- [10] M.L. Wang, T.J. Kretinger, Identification of force from response data of a nonlinear system, *Soil Dynamics and Earthquake Engineering* 13 (1994) 267–280.
- [11] C.H. Huang, An inverse nonlinear force vibration problem of estimating the external forces in a damped system with time-dependent system parameters, *Journal of Sound and Vibration* 242 (2001) 749–765.
- [12] C.K. Ma, P.C. Tuan, D.C. Lin, C.S. Liu, A study of an inverse method for the estimation of impulsive loads, *International Journal of Systems Science* 29 (1998) 663–672.
- [13] E.F. Crawley, A.C. Aubert, Identification of nonlinear structural elements by force-state mapping, *American Institute of Aeronautics and Astronautics Journal* 24 (1986) 155–162.
- [14] H.A. Buchholdt, *Structural Dynamics for Engineers*, Thomas Telford, Springfield, 1997.
- [15] R.E. Kalman, A new approach to linear filtering and prediction problem, *American Society of Mechanical Engineers Journal of Basic Engineering* 82 (1960) 35–45.
- [16] J.M. Mendel, *Lessons in Estimation Theory for Signal Processing, Communications, and Control*, Prentice-Hall PTR, Englewood Cliffs, NJ, 1995.
- [17] M. Gautier, Ph. Poignet, Extended Kalman filtering and weighted least squares dynamic identification of robot, *Control Engineering Practice* 9 (2001) 1361–1372.
- [18] H. Mouri, S. Satoh, H. Furusho, M. Nagai, Investigation of automatic path tracking using an extended Kalman filter, *JSAE Review* 23 (2002) 61–67.
- [19] P.C. Tuan, W.T. Hou, The adaptive robust weighting input estimation method for 1-D inverse heat conduction problems, *Numerical Heat Transfer B* 34 (1998) 319–336.